Synthesis, crystal structure and optical properties of two new layered cadmium iodates: Cd(IO$_3$)X (X=Cl, OH)

Bing-Ping Yang[*], Jiang-Gao Mao

State Key Laboratory of Structural Chemistry, Fujian Institute of Research on the Structure of Matter, Chinese Academy of Sciences, Fuzhou 350002, PR China

ARTICLE INFO

ABSTRACT

Systematic explorations of new compounds in the cadmium iodate system by hydrothermal reactions led to two layered iodates, namely, Cd(IO$_3$)X (X=Cl, OH). Cd(IO$_3$)Cl crystallizes in the orthorhombic space group *Cmca* (No. 64) whereas Cd(IO$_3$)(OH) crystallizes in the orthorhombic space group *Pnma* (No. 62). Cd(IO$_3$)Cl displays a unique double layered structure composed of $_\infty^1$[Cd$-$O$_3$Cl]$_n$ chains. Cadmium octahedrons form a 1D chain along the *a*-axis through edge sharing, and such chains are further interconnected via IO$_3$ groups to form a special double layer on (020) plane. Cd(IO$_3$)(OH) also exhibits a layered structure that is composed of cadmium cations, IO$_3$ groups and hydroxyl ions. Within a layer, chains of CdO$_6$ edge-shared octahedra are observed along the *b*-axis. And these chains are connected by IO$_3$ groups into a layer parallel to the *bc* plane. Spectroscopic characterizations, elemental analysis, and thermogravimetric analysis for the reported two compounds are also presented.

1. Introduction

Noncentrosymmetric (NCS) oxide materials are of current interest owing to their important properties such as second-harmonic generation (SHG) [1], piezoelectricity [2], ferroelectricity [3], and pyroelectricity [4]. Metal iodates can form a diversity of unusual and NCS structures because of the presence of stereo-chemically active lone-pair electrons on I(V) atom which could lead to asymmetric coordination polyhedron [5–9]. The introduction of d^0 transition metal ions such as Ti^{4+}, V^{5+}, Nb^{5+} and Mo^{6+}, which are also susceptible to second-order Jahn–Teller (SOJT) distortion, into the metal iodates, led to a number of novel quaternary iodates [10–24], among which a few compounds have been found to display large SHG responses [10–19]. The introduction of other lone-pair containing cations such as Lead(II) or Bismuth(III) into the metal iodates can also afford materials with excellent SHG properties [25–28]. Recently, we found that combination of d^{10} transition metal cations which are susceptible to Jahn–Teller polarization with d^0 transition metal iodates can also afford new second-order NLO compounds [29]. As for metal iodates of cadmium, δ-Cd(IO$_3$)$_2$ that crystallizes in a non-centrosymmetric space group $P2_12_12_1$ has been prepared [30]. Another polymorphism ε-Cd(IO$_3$)$_2$ is also structurally non-centrosymmetric and belong to space group $Pca2_1$ [31]. Centrosymmetric Cd(IO$_3$)$_2$(H$_2$O) has also

been reported [32]. Our current research interests focus on the effects of the other anions such as chlorine ions and hydroxyl ions on the structures of compounds formed in the cadmium iodates system. Only a few iodate–chlorides [33–37] or iodate–hydroxides [6,18,22,38–41] have been structurally described. So far, no cadmium iodate with chlorine or hydroxyl ion has been reported. Our research efforts led to two new layered cadmium iodates, namely, Cd(IO$_3$)X (X=Cl, OH). Herein, we report their syntheses, crystal structures and characterizations.

2. Experimental section

2.1. Materials and methods

All of the chemicals were analytically pure from commercial sources and used without further purification. CdCl$_2$ (≥98%), Cd (CH$_3$COO)$_2 \cdot$ 2H$_2$O (≥99%), K$_2$CO$_3$ (≥99%) and I$_2$O$_5$ (≥99%) were purchased from the Shanghai Reagent Factory. Microprobe elemental analyses were performed on a field emission scanning electron microscope (FESEM, JSM6700F) equipped with an energy dispersive X-ray spectroscope (EDS, Oxford INCA). The X-ray powder diffraction data were collected on a Rigaku MiniFlexII diffractometer using graphite-monochromated Cu-Ka radiation in the 2θ range of 5–65° with a step size of 0.05° (Fig. 4). TGA and DTA studies were all carried out with a NETZSCH STA 449C or 449F3 instruments. The sample and reference (Al$_2$O$_3$) were enclosed in a platinum crucible and heated at a rate of 15 °C/min

* Corresponding author. Tel.: +86 591 83736672; fax: +86 591 83714946.
E-mail address: ybp@fjirsm.ac.cn (B.-P. Yang).

from room temperature to 1000 °C under a nitrogen atmosphere. The IR spectra were recorded on a BRUKER OPTICS VERTEX 70 FT-IR spectrometer as KBr pellets in the range of 4000–400 cm^{-1}. The UV–vis–NIR absorption and optical diffuse reflectance spectra were measured at room temperature with a PE Lambda 900 UV–vis–NIR spectrophotometer in the range of 190–2500 nm. BaSO$_4$ plate was used as a standard (100% reflectance). The absorption spectrum was calculated from reflectance spectrum using the Kubelka–Munk function [42]: $\alpha/S=(1-R)^2/2R$, where α is the absorption coefficient, S is the scattering coefficient which is practically wavelength independent when the particle size is larger than 5 μm, and R is the reflectance.

2.2. Synthesis

Single crystals of Cd(IO$_3$)Cl were synthesized by the hydrothermal reactions of a mixture of CdCl$_2$ (0.1833 g, 1 mmol), I$_2$O$_5$ (0.1669 g, 0.5 mmol), and 1 ml of water sealed in an autoclave equipped with a Teflon liner (23 mL) at 200 °C for 4 days, and then cooled to 30 °C at 6 °C/h. The final reaction products were washed with water and ethanol, and then dried in air. Colorless prism shaped single crystals of Cd(IO$_3$)Cl were collected in a yield of 82% based on Cd as pure phase. The initial and final pH values of the reaction media are 2 and 1, respectively. Cd(IO$_3$)(OH) was synthesized by a similar method. The loaded compositions are Cd(CH$_3$COO)$_2 \cdot$ 2H$_2$O (0.0666 g, 0.25 mmol), I$_2$O$_5$ (0.2086 g, 2.5 mmol), K$_2$CO$_3$ (0.0345 g, 0.625 mmol), and H$_2$O (3 ml). The initial and final pH values of the reaction media are 6 and 7. Colorless platelike single crystals of Cd(IO$_3$)(OH) were collected in a ca 86% yield based on Cd. Microprobe elemental analyses were performed on several single crystals of each compound. The average molar ratio of Cd:I:Cl was 1.0:1.1:0.9 for Cd(IO$_3$)Cl, the ratio of Cd:I was 1.0:0.9 for Cd(IO$_3$)(OH). These elemental analyses data are in good agreement with those determined from single-crystal X-ray structural studies.

2.3. Single crystal X-ray diffraction

Crystallographic data of Cd(IO$_3$)Cl were collected on a SCXmini CCD diffractometer equipped with a graphite-monochromated Mo-Kα radiation ($\lambda=0.71073$ Å) at 293 K. Crystallographic data of Cd(IO$_3$)(OH) were collected on a SuperNova X-ray diffractometer. The data sets were corrected for Lorentz and polarization factors as well as for absorption by SADABS program [43]. All structures were solved by the direct method and refined by full-matrix least-squares fitting on F^2 by SHELX-97 [43]. All non-hydrogen atoms were refined with anisotropic thermal parameters. Hydrogen atom in Cd(IO$_3$)(OH) was not refined due to the difficulty in the determination of its exact location. Crystallographic data and structural refinements for the two compounds are summarized in Table 1. Important bond lengths are listed in Table 2. Further details of the crystal structure investigations can be obtained from the Fachinformationszentrum Karlsruhe, 76344 Eggenstein-Leopoldshafen, Germany (fax: +49 7247808666; e-mail: crysdata@fiz-karlsruhe.de), on quoting the depository numbers CSD – 422802 and 427792.

2.4. Computational descriptions

Single-crystal structural data of Cd(IO$_3$)Cl was used for the theoretical calculations. The ab initio band structure calculations and density of states (DOS) were performed by using the computer code CASTEP [44,45]. The total energy was calculated within the framework of nonlocal gradient-corrected approximations [Perdew–Burke–Ernzerhof (PBE) functional] [46]. The interactions between the ionic cores and the electrons were described by the ultrasoft pseudopotentials [47]. The number of plane waves included in the basis set was determined by a cutoff energy of

Table 1
Crystallographic data for Cd(IO$_3$)Cl and Cd(IO$_3$)(OH).

Compound	Cd(IO$_3$)Cl	Cd(IO$_3$)(OH)
Fw	322.75	304.31
Space group	Cmca (No. 64)	Pnma (No. 62)
a, Å	7.293(6)	11.5245(11)
b, Å	16.04(2)	6.7985(7)
c, Å	7.207(5)	4.7303(4)
V, Å^3	843(1)	370.62(6)
Z	8	4
D_{calc}, g cm^{-3}	5.086	5.454
μ, mm^{-1}	12.987	14.074
GOF	1.175	1.086
R1[a], wR2[b] [$I > 2\sigma(I)$]	0.0157, 0.0373	0.0361, 0.0921
R1, wR2 (all data)	0.0165, 0.0378	0.0430, 0.1009

[a] $R_1 = \sum ||Fo| - |Fc||/\sum |Fo|$,
[b] $wR_2 = \{\sum w[(Fo)^2 - (Fc)^2]^2/\sum w[(Fo)^2]^2\}^{1/2}$.

Table 2
Selected bond lengths (Å) for Cd(IO$_3$)Cl and Cd(IO$_3$)(OH).

Cd(IO$_3$)Cl			
Cd(1)-O(1)	2.308(3)	Cd(1)-Cl(1)	2.5662(16)
Cd(1)-O(1)#1	2.308(3)	Cd(1)-Cl(1)#4	2.5662(16)
Cd(1)-O(2)#2	2.314(2)	I(1)-O(1)	1.813(2)
Cd(1)-O(2)#3	2.314(2)	I(1)-O(1)#6	1.813(2)
		I(1)-O(2)	1.833(3)
Cd(IO$_3$)(OH)			
Cd(1)-O(3)#1	2.240(4)	Cd(1)-O(1)#4	2.328(5)
Cd(1)-O(3)	2.240(4)	Cd(1)-O(1)#5	2.328(5)
Cd(1)-O(2)#2	2.323(4)	I(1)-O(1)	1.797(4)
Cd(1)-O(2)#3	2.323(4)	I(1)-O(1)#8	1.797(4)
		I(1)-O(2)	1.864(7)

Symmetry transformations used to generate equivalent atoms: #1 $-x+1/2,y+0,$ $-z+1/2$ #2 $-x,-y,-z$ #3 $-x+1/2,-y+0,z+1/2$ #4 $x-1/2,-z+1/2$ #6 $-x,y,z$ for Cd(IO$_3$)Cl; #1 $-x+1,-y+1,-z$ #2 $x-1/2,y,-z-1/2$ #3 $-x+3/2,-y+1,z+1/2$ #4 $-x+3/2,-y+1,z-1/2$ #5 $x-1/2,y,-z+1/2$ #8 $x,-y+1/2,z$ for Cd(IO$_3$)(OH).

340 eV. The numerical integration of the Brillouin zone was performed by using $3 \times 2 \times 3$ Monkhorst-Pack k-point sampling. The following orbital electrons were treated as valence electrons: Cd-4d^{10}5s^{2}5p^0, Cl-3s^{2}3p^5, I-5s^{2}5p^5 and O-2s^{2}2p^4. The other calculating parameters used in the calculations and convergent criteria were set by the default values of the CASTEP code.

3. Results and discussion

3.1. Structural description

Cd(IO$_3$)Cl and Cd(IO$_3$)(OH) both exhibit two-dimensional layered structures. But the layers in two compounds are quite distinct due to the different auxiliary anion ligand. We will discuss the structure in detail.

Cd(IO$_3$)Cl displays a special double-layered structure composed of [CdO$_3$Cl]$_n$ chains (see Fig. 1(a)). The Cd cation is in a distorted octahedral geometry [CdO$_4$Cl$_2$], being coordinated by four oxygen atoms from four iodate groups (Cd–O 2.308(3) − 2.314(2) Å) and two chlorine anions (Cd–Cl 2.566(2) Å). Both I^{5+} cations are coordinated by three oxygen atoms in a distorted trigonal–pyramidal geometry. I–O distances are in the range of 1.813(2)–1.833(3) Å, which are comparable to other iodates. Chlorine anions act as μ^2 linkages with Cd(1)–Cl(1)–Cd(1) angle of 90.55(7)°.

[CdO$_4$Cl$_2$] octahedra are linked into a chain along the a-axis through edge sharing (O(2)Cl(1)), these chains are further interconnected by IO$_3$ groups into a special double layer on the (020) plane (Fig. 2(a) and (b)). The Cd$\cdots$Cd separation in a chain is 3.646(3) Å. The interlayer distance is 8.020(7) Å. Each IO$_3$ group is

quadridentate, it bridges with four Cd atoms. Two oxygen atoms are unidentate whereas the third one (O(2)) is bidentate. The polarizations of IO_3 groups are canceled each other, hence the compound is non-polar (Fig. 3(a)). Results of bond valence calculations indicate that Cd and I atoms are in oxidation states of $+2$ and $+5$ respectively [48,49]. The calculated total bond valences are 2.099 and 4.886 for Cd(1) and I(1), respectively.

The asymmetric unit of $Cd(IO_3)(OH)$ contains one Cd, one I, two O atoms and one hydroxyl ligand. The O(1) atom occupies the general position, whereas other atoms are located on sites of two-fold symmetry. Cd(1) is in a distorted octahedral geometry CdO_6, being coordinated by six oxygen atoms from four iodate groups (Cd–O 2.323(4) – 2.328(5) Å) and two hydroxyl ions (Cd–O(3) 2.240(4) Å). I(1) is coordinated by three oxygen atoms in a distorted trigonal–pyramidal geometry with I–O bond length in the range of 1.797(4) – 1.864(7) Å. Oxygen atom O(3) of the hydroxyl ion links two Cd cations with Cd(1)–O(3)–Cd(1) angle of 98.7(3)°. These Cd–O and I–O distances are in good agreement with the literature values.

CdO_6 octahedrons share edges (O(2) of iodate groups and O (3) of hydroxyl ions) into a chain (Fig. 1(b)). These chains are further interconnected by IO_3 groups into a layer parallel to (200)

plane (Fig. 2(c) and (d)). Results of bond valence calculations indicate that Cd and I atoms are in oxidation states of $+2$ and $+5$ respectively. The calculated total bond valences are 2.807, and 4.906 for Cd(1) and I(1) respectively. The calculated bond valence of O(3) which connected to H^+ ion is 1.075.

Comparison of the two compounds, the primary reason of distinct structure is the different size of chlorine ion and hydroxyl group. They both act as μ^2 linkages, but they have distinct bond lengths and angles. Cd–Cl bond length 2.566(2) Å is much longer than the Cd–O(H) bond length 2.240(4) Å, and Cd(1)–Cl(1)–Cd (1) bond angle 90.55(7)° is smaller than Cd(1)–O(H)–Cd(1) angle 98.7(3)°. Cl–Cd–Cl bond angle in the $[CdO_3Cl]_n$ chain of $Cd(IO_3)Cl$ is 96.9° whereas (H)O–Cd–O(H) bond angle in the $[CdO_3OH]_n$ chain of $Cd(IO_3)(OH)$ is 180°. In other words, chlorine anions are located in the same side of the chain, but hydroxyl ions alternately lie in opposite sides of the chain. So $Cd(IO_3)Cl$ features a unique double layered structure whereas $Cd(IO_3)(OH)$ displays an ordinary layered structure.

It is worthy to compare the structure with those of other cadmium iodates. δ-$Cd(IO_3)_2$ ($P2_12_12_1$) features a 2D layer structure in which CdO_7 polyhedra are linked into a chain through vertex sharing. ε-$Cd(IO_3)_2$ ($Pca2_1$) features a 3D framework in which two cadmium polyhedrons units are linked through iodate bridges resulting in layers parallel to the (100) plane, layers are further linked by the other iodate groups into a 3D framework. The structure of $Cd(IO_3)_2 \cdot H_2O$ consists of Cd_2O_2 dimers which are connected through two iodate bridges resulting in layers parallel to the (010) plane. Comparing with $Zn(IO_3)(OH)$ which features a layered structure that is composed of ZnO_6 and IO_3 polyhedra [41]. It is worth mentioning that Cd–O–Cl and Cd–O chains of $Cd(IO_3)X$ (X=Cl, OH) are similar to Zn–O chains in $Zn(IO_3)(OH)$. The difference is Cl–Cd–Cl bond angle is 96.9°, (H)O–Cd–O(H) bond angle is 180°, whereas (H) O–Zn–O(H) bond angle is 134°. Hydroxyl ions are almost located in the same side of the Zn–O chain of the $Zn(IO_3)(OH)$. The lone pairs on I^{5+} cations approximately point in the $[01-1]$ and $[0-1-1]$ directions, so a small moment in the [001] direction produces and $Zn(IO_3)(OH)$ shows a mild SHG efficiency. In $Cd(IO_3)(OH)$, the lone pairs on IO_3 polyhedra are oriented in opposite directions which result in the cancellation of the local dipole moments, rendering the materials nonpolar.
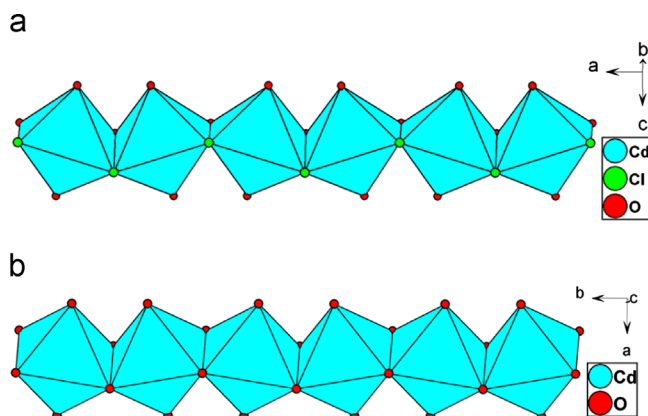

Fig. 1. View of the chain of $Cd(IO_3)Cl$ (a) and $Cd(IO_3)(OH)$ (b).
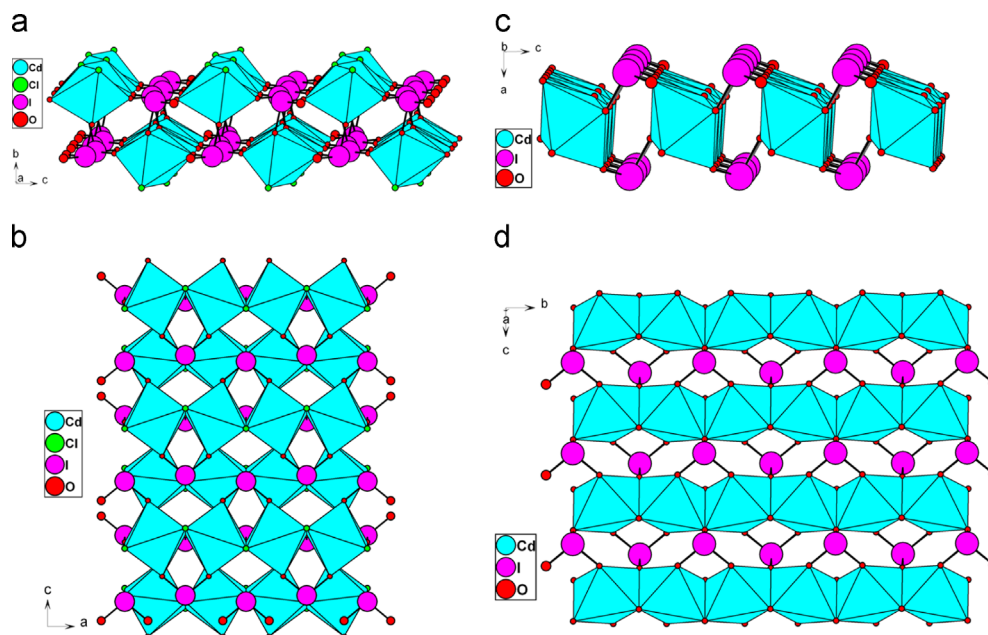
Fig. 2. View of the 2D layer of $Cd(IO_3)Cl$ (a) (b) and $Cd(IO_3)(OH)$ (c) (d) along the [100] and [010] direction.
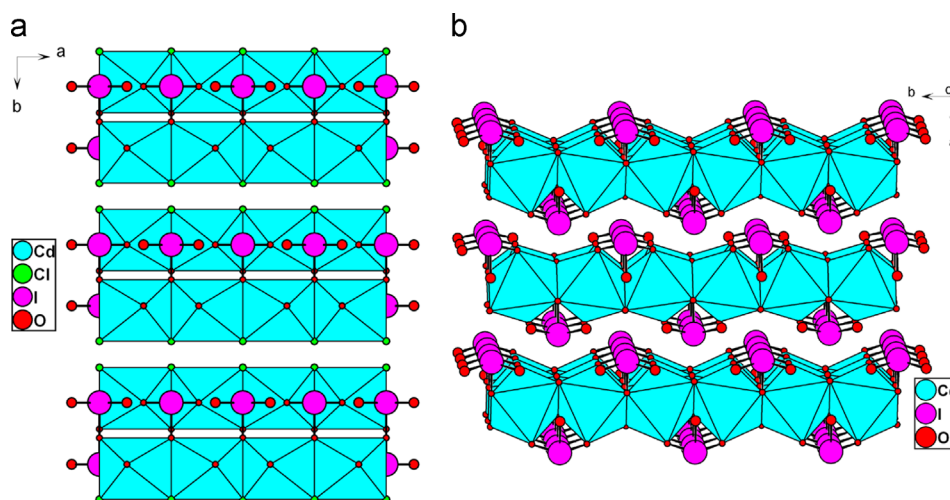
Fig. 3. View of the 3D packing of $Cd(IO_3)Cl$ (a) and $Cd(IO_3)(OH)$ (b) along the [001] direction.

3.2. Characterizations

Results of TGA studies indicate that $Cd(IO_3)Cl$ is stable up to 510 °C, upon further heating, the iodate groups and chlorine ions start to decompose through thermal disproportionation which end at about 690 °C. These assignments are in agreement with the endothermic peak at 526 °C in the DTA diagram (Fig. 5(a)). $Cd(IO_3)$(OH) exhibits two distinct weight loss steps. The first weight loss occurs at 360–420 °C, which corresponds to losing OH groups. And the second step, occurring between 500 and 700 °C, can be attributed to decomposing of iodate groups. These assignments are in agreement with the small endothermic peak at 380 °C and the large and broad endothermic peak around 586 °C in the DSC diagram for $Cd(IO_3)(OH)$ (Fig. 5(b)). The thermal behavior of $Cd(IO_3)(OH)$ is very similar to that of $ZnIO_3(OH)$ [41].

IR spectra of two compounds show the symmetric ($\nu 1$) and anti-symmetric ($\nu 3$) IO_3^- stretching bands in the range $701 - 815 \, cm^{-1}$ (Fig. 6). In the diagram of $Cd(IO_3)(OH)$, a sharp peak at $3492 \, cm^{-1}$ corresponds to the stretching vibration of the hydroxyl group. The assignments are consistent with the previously reported compound $ZnIO_3(OH)$.

UV–vis–NIR absorption spectrum of $Cd(IO_3)Cl$ shows little absorption in the range of 320–2500 nm (0.32–2.5 μm). UV–vis–NIR absorption spectrum of $Cd(IO_3)(OH)$ displays some absorption bands in the range of 1400–2500 nm which may be originated from characteristic hydroxyl O–H stretching vibrations (Fig. 7).

Optical diffuse reflectance spectra studies indicate that $Cd(IO_3)$Cl and $Cd(IO_3)(OH)$ are insulators with optical band gaps of 4.3 and 4.35 eV which are determined from the extrapolation of the absorption edge to the baseline (Fig. S1).

3.3. Theoretical studies

To further understand the chemical bonding in the compound $Cd(IO_3)Cl$, band structure as well as DOS calculations based on the DFT method were made by using the computer code CASTEP.

The calculated band structures of the compound along high-symmetry points of the first Brillouin zone are plotted in Fig. S2. For $Cd(IO_3)Cl$, the lowest energy of conduction band (L-CB) is at G point and the highest energy of valence band (H-VB) is between G and S, thus it is an indirect band-gap crystal with a band gap of 3.27 eV (Table S1). The calculated band gap is much smaller than the experimental value (4.35 eV). It is well known that the DFT–GGA does not accurately describe the eigenvalues of the electronic states, causing the quantitative underestimation of band gaps [50].
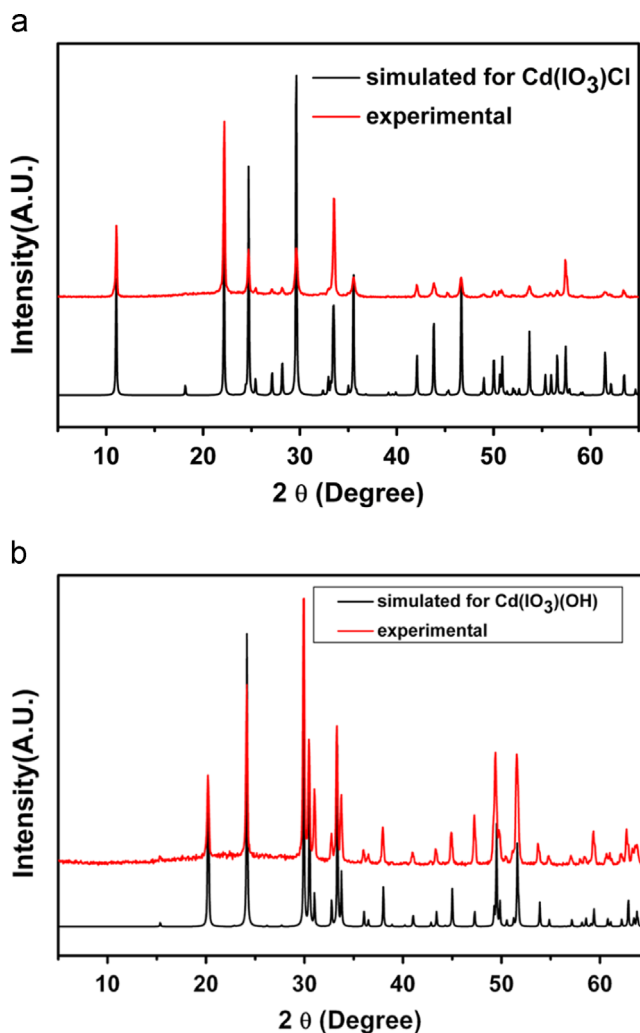

Fig. 4. X-ray diffraction powder patterns for $Cd(IO_3)Cl$ (a) and $Cd(IO_3)(OH)$ (b).

The bands can be assigned according to the total and partial densities of states (DOS) as plotted in Fig. S3. The bottommost VB region around -20 eV comes from O-2s and I-5s states, and the bands between -18 and -16.5 eV are mainly originated from O-2s states, mixing with small amount of 5p states. Isolated Cl-3s
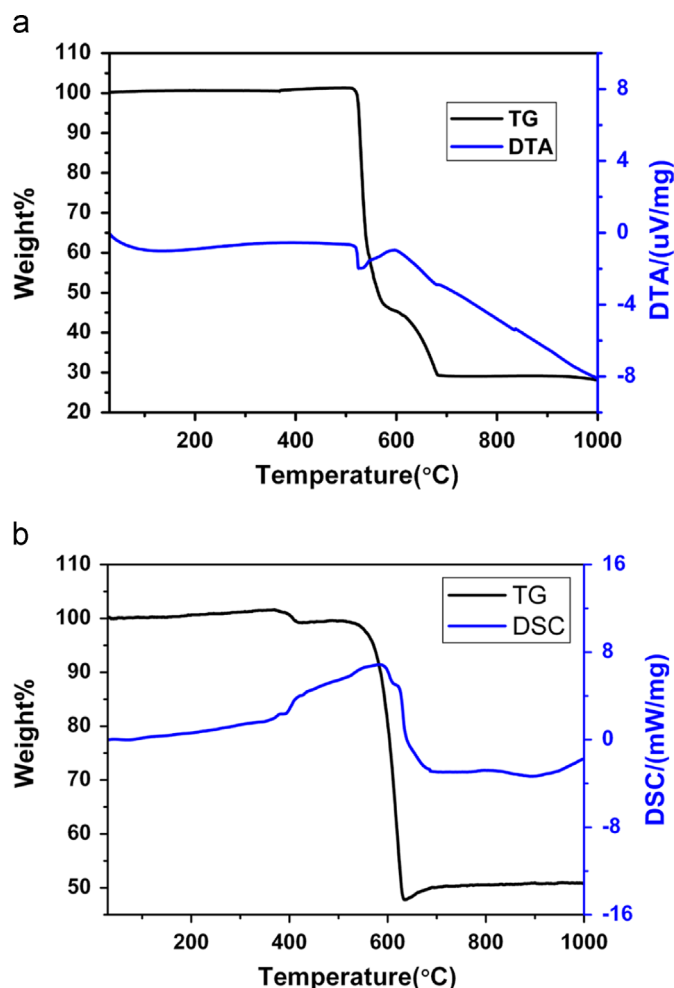
a

b

Fig. 5. TG and DTA diagrams for Cd(IO$_3$)Cl (a), TG and DSC diagrams for Cd(IO$_3$)(OH) (b).
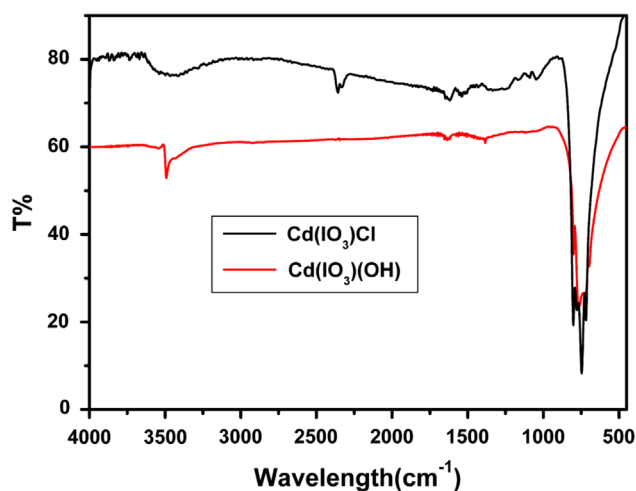
Fig. 6. Infrared spectra for Cd(IO$_3$)Cl and Cd(IO$_3$)(OH).

states contribute to the peak near -13 eV. The bands from -11.7 to -9.9 eV are composed of I-5s and O-2s states. In the Fermi level regions, namely, -7.5–0 eV in VB, the overlap of O-2p, I-5p, Cd-4d and Cl-3p, indicate the covalent interactions between them. The bands above the Fermi level (3.2–7.5 eV) are predominately derived from I-5p and O-2p states. In addition, the CB from 7.6 to 13 eV arises from Cd-5s, 5p, I-5s, and some O-2p, Cl-3p states.
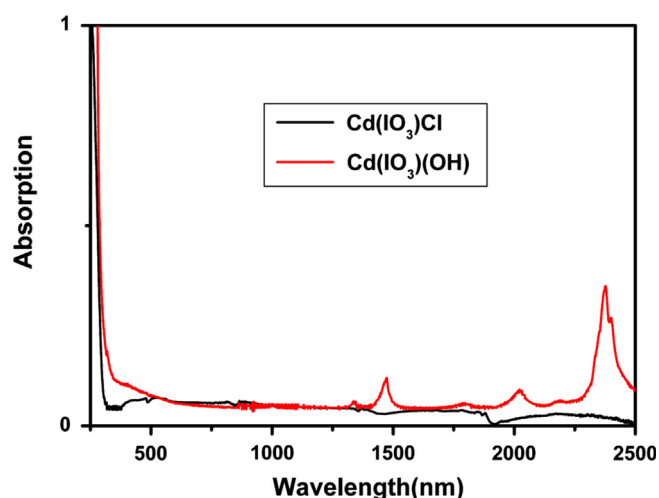

Fig. 7. UV–vis–NIR absorption spectra for Cd(IO$_3$)Cl and Cd(IO$_3$)(OH).

Population analyses allow for a more quantitative bond analysis. The calculated bond orders of Cd–O, Cd–Cl and I–O bonds are 0.16–0.22 e, 0.29 e and 0.33–0.34 e, respectively (covalent single-bond order is generally 1.0 e), so we can say that I–O bonds have more covalent character (see Table S2).

4. Conclusions

In summary, two new layered cadmium iodates with chlorine or hydroxyl ion, namely, Cd(IO$_3$)X (X=Cl, OH), have been synthesized and characterized. They both exhibit two-dimensional layered structures. But the layers in two compounds are quite distinct. We deem that the primary reason of distinct structure is the different size of chlorine ion and hydroxyl group. Optical properties characterizations, elemental analysis, and thermogravimetric analysis have been performed on the reported two compounds. Since these structures are centrosymmetric, the compounds are not SHG active, but this does not rule out the possibility to find SHG materials in the cadmium iodate system. Our future research efforts will be devoted to further studies on the syntheses, crystal structures and optical properties of other related phases.

Appendix A. Supporting information

Supporting information associated with this article can be found in the online version at http://dx.doi.org/10.1016/j.jssc.2014.07.032.

References

[1] K. Zhang, X. Wang, Nonlinear Optical Crystal Materials Science, Science Press, Peking, 1996.
[2] W.G. Cady, Piezoelectricity: an Introduction to the Theory and Applications of Electromechanical Phenomena in Crystals, Dover, New York, 1964.
[3] F. Jona, G. Shirane, Ferroelectric Crystals, Pergamon Press, Oxford, U.K., 1962.
[4] S.B. Lang, Sourcebook of Pyroelectricity, Gordon & Breach Science, London, 1974.
[5] K.M. Ok, P.S. Halasyamani, Angew. Chem.-Int. Ed. 43 (2004) 5489–5491.
[6] K.M. Ok, P.S. Halasyamani, Inorg. Chem. 44 (2005) 9353–9359.
[7] D. Phanon, I. Gautier-Luneau, Angew. Chem.-Int. Ed. 46 (2007) 8488–8491.
[8] D. Phanon, A. Mosset, I. Gautier-Luneau, J. Mater. Chem. 17 (2007) 1123–1130.
[9] X. Xu, B.P. Yang, C. Huang, J.G. Mao, Inorg. Chem. 53 (2014) 1756–1763.

[10] H.Y. Chang, S.H. Kim, P.S. Halasyamani, K.M. Ok, J. Am. Chem. Soc. 131 (2009) 2426–2427.
[11] H.Y. Chang, S.H. Kim, K.M. Ok, P.S. Halasyamani, J. Am. Chem. Soc. 131 (2009) 6865–6873.
[12] R.E. Sykora, K.M. Ok, P.S. Halasyamani, D.M. Wells, T.E. Albrecht-Schmitt, Chem. Mater. 14 (2002) 2741–2749.
[13] B.P. Yang, C.L. Hu, X. Xu, C.F. Sun, J.H. Zhang, J.G. Mao, Chem. Mater. 22 (2010) 1545–1550.
[14] C.-F. Sun, C.-L. Hu, X. Xu, B.-P. Yang, J.-G. Mao, J. Am. Chem. Soc. 133 (2011) 5561–5572.
[15] C. Huang, C.L. Hu, X. Xu, B.P. Yang, J.G. Mao, Dalton Trans. 42 (2013) 7051–7058.
[16] C.F. Sun, C.L. Hu, X. Xu, J.B. Ling, T. Hu, F. Kong, X.F. Long, J.G. Mao, J. Am. Chem. Soc. 131 (2009) 9486–9487.
[17] R.E. Sykora, K.M. Ok, P.S. Halasyamani, T.E. Albrecht-Schmitt, J. Am. Chem. Soc. 124 (2002) 1951–1957.
[18] T.C. Shehee, R.E. Sykora, M.K. Kang, P.S. Halasyamani, T.E. Albrecht-Schmitt, Inorg. Chem. 42 (2003) 457–462.
[19] X.A. Chen, L. Zhang, X.N. Chang, H.P. Xue, H.G. Zang, W.Q. Xiao, X.M. Song, H. Yan, J. Alloy. Compd. 428 (2007) 54–58.
[20] C.F. Sun, C.L. Hu, F. Kong, B.P. Yang, J.G. Mao, Dalton Trans. 39 (2010) 1473–1479.
[21] B.-P. Yang, X. Xu, C. Huang, J.-G. Mao, CrystEngComm 15 (2013) 10464–10469.
[22] X.A. Chen, X.A. Chang, H.G. Zang, Q. Wang, W.Q. Xiao, J. Alloy. Compd. 396 (2005) 255–259.
[23] C.F. Sun, T. Hu, X. Xu, J.G. Mao, Dalton Trans. 39 (2010) 7960–7967.
[24] R.E. Sykora, S.M. McDaniel, D.M. Wells, T.E. Albrecht-Schmitt, Inorg. Chem. 41 (2002) 5126–5132.
[25] T. Hu, L. Qin, F. Kong, Y. Zhou, J.G. Mao, Inorg. Chem. 48 (2009) 2193–2199.
[26] S.D. Nguyen, J. Yeon, S.-H. Kim, P.S. Halasyamani, J. Am. Chem. Soc. 133 (2011) 12422–12425.
[27] Z.B. Cao, Y.C. Yue, J.Y. Yao, Z.S. Lin, R. He, Z.G. Hu, Inorg. Chem. 50 (2011) 12818–12822.
[28] C.F. Sun, C.L. Hu, J.G. Mao, Chem. Commun. 48 (2012) 4220–4222.
[29] B.P. Yang, C.L. Hu, X. Xu, C. Huang, J.G. Mao, Inorg. Chem. 52 (2013) 5378–5384.
[30] H. Bach, H. Kuppers, Acta Crystallogr. B 34 (1978) 263–265.
[31] B. Bentria, D. Benbertal, Z. Hebboul, M. Bagieu-Beucher, A. Mosset, Z. Anorg. Allg. Chem. 631 (2005) 894–901.
[32] B. Bentria, D. Benbertal, M. Bagieu-Beucher, A. Mosset, Z. Anorg. Allg. Chem. 630 (2004) 781–782.
[33] A.M. Lanfredi, A Tiripicc, Ma Pellingh, Acta Crystall. B-Struct. B 28 (1972) 1822–1826.
[34] A.C. Bean, Y.W. Xu, J.A. Danis, T.E. Albrecht-Schmitt, B.L. Scott, W. Runde, Inorg. Chem. 41 (2002) 6775–6779.
[35] R.P. Sharma, R. Bala, R. Sharma, V. Ferretti, Inorg. Chim. Acta 358 (2005) 3457–3464.
[36] E.L. Belokoneva, O.V. Dimitrova, Crystallogr. Rep. 55 (2010) 24–27.
[37] W.W. Zhao, S.L. Pan, L.Y. Dong, Z.H. Yang, X.Y. Dong, Z.H. Chen, M. Zhang F.F. Zhang, J. Mol. Struct. 1049 (2013) 288–292.
[38] S. Ghose, C. Wan, Am. Mineral. 63 (1978) 172–179.
[39] L. Zhang, X. Chen, X. Chang, H. Zang, W. Xiao, J. Synthetic Cryst. 34 (2005) 812–816.
[40] X.M. Liu, G.H. Li, Y.W. Hu, M. Yang, X.G. Kong, Z. Shi, S.H. Feng, Cryst. Growth Des. 8 (2008) 2453–2457.
[41] D.W. Lee, S.B. Kim, K.M. Ok, Dalton Trans. 41 (2012) 8348–8353.
[42] W.W.M. Wendlandt, H.G. Hecht, Reflectance Spectroscopy, Wiley, New York, 1966.
[43] G.M. Sheldrick, SHELXTL, Crystallographic Software Package, Version 5.1, Bruker-AXS, Madison, WI, 1998.
[44] M.D. Segall, P.J.D. Lindan, M.J. Probert, C.J. Pickard, P.J. Hasnip, S.J. Clark M.C. Payne, J. Phys.-Condens. Matter 14 (2002) 2717–2744.
[45] V. Milman, B. Winkler, J.A. White, C.J. Pickard, M.C. Payne, E.V. Akhmatskaya, R.H. Nobes, Int. J. Quantum Chem. 77 (2000) 895–910.
[46] J.P. Perdew, K. Burke, M. Ernzerhof, Phys. Rev. Lett. 77 (1996) 3865–3868.
[47] D. Vanderbilt, Phys. Rev. B 41 (1990) 7892–7895.
[48] I.D. Brown, D. Altermatt, Acta Crystallogr. B 41 (1985) 244–247.
[49] N.E. Brese, M. Okeeffe, Acta Crystallogr. B 47 (1991) 192–197.
[50] C.M.I. Okoye, J. Phys.-Condens. Matter 15 (2003) 5945–5958.